Reports

Radio Tracking of Solar Energetic Particles through Interplanetary Space

Abstract. *Energetic particles ejected from the sun generate radio waves as they travel out through the interplanetary medium. Satellite observations of this emission at long radio wavelengths provide a means of investigating properties of the interplanetary medium, including the gross magnetic field configuration over distances of 1 astronomical unit. Results of such observations are illustrated.*

Satellite observations of traveling solar radio bursts provide information about the propagation of energetic solar particles through interplanetary space. This, in turn, leads to data on the solar wind density and gross magnetic field configuration over distances of 1 A.U. In this report we illustrate some of these results and, in particular, show the first "radio picture" over 1 A.U. of the spiral magnetic field configuration in interplanetary space.

Because of the general supersonic coronal expansion (*1*), called the solar wind, the magnetic field lines from the solar surface are stretched out into the interplanetary medium. However, the solar rotation twists the magnetic lines so that the resulting pattern in interplanetary space should be an Archimedean spiral under quiet solar conditions. The solar wind model developed by Parker (*1*) has been confirmed near the earth by satellite observations. Wilcox (*2*) has reviewed the space probe measurements of the interplanetary magnetic field.

We know that among the energetic particles ejected from the sun there are packets and streams of superthermal electrons, with energies of the order of tens of thousands of electron volts (*3*). These electrons are ejected not only at the times of large flares but also on occasions of less energetic disturbances, and indeed even when no flare is observed optically. Because the energy density of the packet or stream of superthermal electrons is small compared to that of the solar wind and since the electron gyroradius is small, the electrons will be "guided" by the magnetic field lines. Therefore, the observation of the electron propagation should provide an excellent method of tracing out the magnetic field configuration.

Since the superthermal electrons generate radio emission, their propagation path through interplanetary space can, in fact, be observed in a fashion analogous to the way the ionization trail of a charged particle illuminates its path in a cloud or bubble chamber. As the superthermal electrons travel out through the solar wind, they excite the medium through which they pass. Cerenkov plasma waves are set up in the medium at a frequency determined by the local density (*4*). Part of this energy is converted at a frequency characteristic of that coronal level into radio waves which can propagate to a remote observing point. This type of solar radio process is called a fast drift (type III) event and is characterized

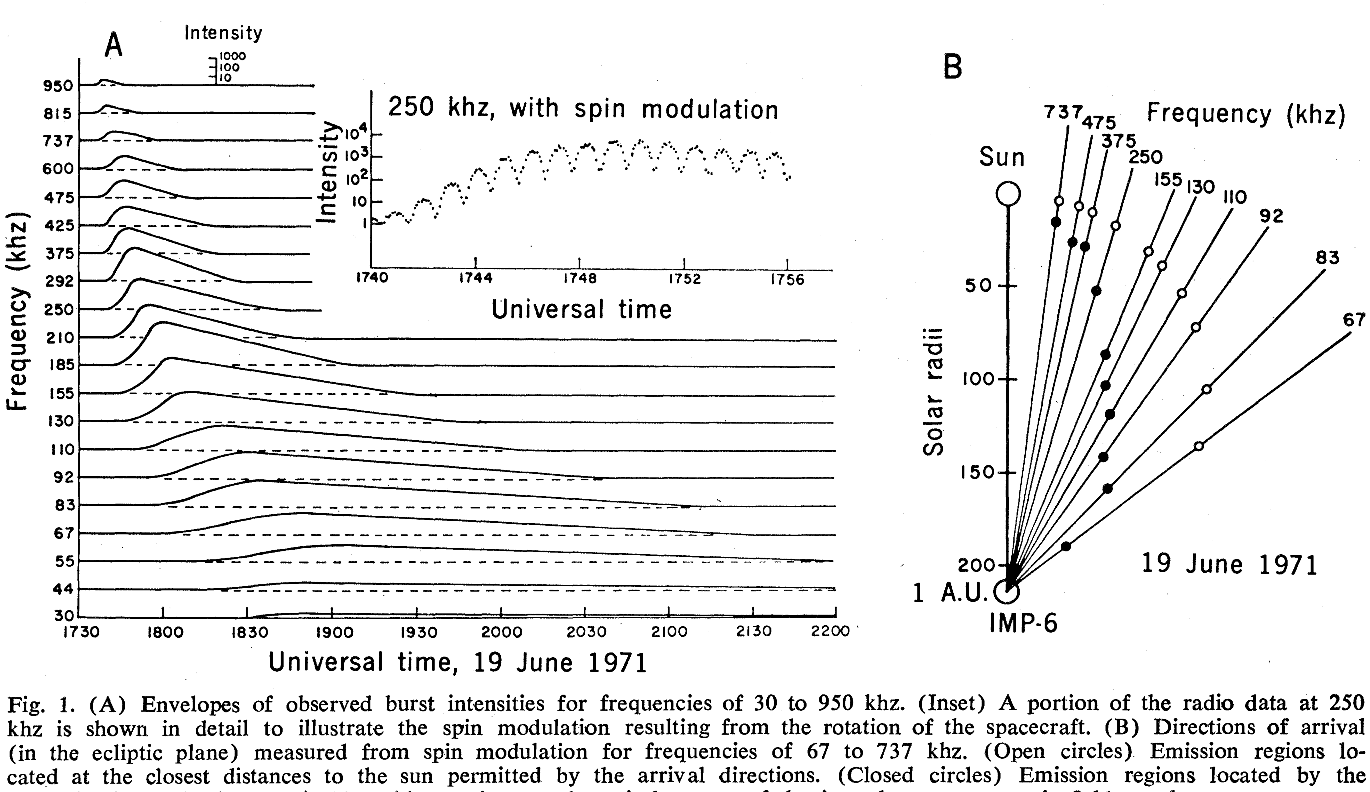

Fig. 1. (A) Envelopes of observed burst intensities for frequencies of 30 to 950 khz. (Inset) A portion of the radio data at 250 khz is shown in detail to illustrate the spin modulation resulting from the rotation of the spacecraft. (B) Directions of arrival (in the ecliptic plane) measured from spin modulation for frequencies of 67 to 737 khz. (Open circles) Emission regions located at the closest distances to the sun permitted by the arrival directions. (Closed circles) Emission regions located by the RAE density scale (see text). For either trajectory the spiral nature of the interplanetary magnetic field can be seen.

by dynamic spectra showing a drift in time from high to low frequencies because of the outward motion of the exciter from regions of high density near the sun to regions of lower density.

Ground-based radio telescopes can see through the terrestrial ionosphere down to frequencies of the order of 20 Mhz so that these type III bursts can be observed only out to distances of a few solar radii from the sun. Placing a radio telescope well above the ionosphere makes it possible to observe the radio emission down to frequencies that correspond to emission at distances of the order of 215 solar radii or 1 A.U. The observations reported here were obtained with a radio telescope flown on the Interplanetary Monitoring Platform IMP-6. The receiver samples sequentially 39 frequencies in the range from 10 Mhz to 30 khz. The antenna is a dipole 92 meters long. Because the beam width of this antenna is broad, its angular resolution is normally inadequate for tracking the radio source. However, the spacecraft is spin stabilized so that the dipole reception pattern, with its nulls, is swept past the source direction many times during the duration of a burst. By utilizing the spin modulation of the received data and the null of the reception pattern, the direction of a compact source can be detected. In a more accurate method used in this experiment the known dipole pattern is cross-correlated with the received modulation data. The phase is adjusted until maximum correlation occurs, and this phase can be simply related to the direction of the source relative to a reference direction, such as the center of the sun. In addition, the source size can be estimated from the depth of modulation; for larger source sizes, the reception pattern null is "filled in" and the percentage of modulation decreases. Thus, the spinning dipole provides a means of determining the direction of arrival and an estimate of the size of the source. A complete error analysis of the method has been made and indicates that with 50 data samples (approximately 3 minutes of data) the average source position can be determined within an accuracy of 1° for small sources near the spin plane.

An observation of a burst down to low frequencies on 19 June 1971 by the IMP-6 satellite is illustrated in Fig. 1A, where the envelopes of the burst and an example of the spin modulated data recorded at one frequency are plotted. Figure 1B shows the directions of arrival obtained from the modulation patterns at the indicated frequencies for the event of 19 June. Above 737 khz the burst intensity was too small to yield a direction, and below 67 khz the level of modulation was not sufficient to yield a direction.

In order to determine the trajectory of the particles, a relationship is also needed between electron density and distance from the sun. We used two models for locating the emission regions. In the first model, we used the density-distance scale obtained from radio observations of the Radio Astronomy Explorer (RAE) satellite (*5*) in the range from 10 to 40 solar radii, and extrapolated the scale to 1 A.U. In the second model, we placed the emission regions at coronal levels equal to the minimum distances from the sun permitted by the measured directions of arrival. The two sets of points obtained (see Fig. 1B) represent reasonable bounds on the particle trajectories, and both sets determine a spiral magnetic field configuration expected under average conditions.

The positions of the radio emission shown in Fig. 1B can be compared to the plot of interplanetary density against distance shown in Fig. 2A. The lower line is a density scale interpolated between values at 10 solar radii and at 1 A.U. The value of 10^4 cm^{-3} at 10 solar radii was obtained from observations of light scattering (*6*). The value of 5 cm^{-3} at 1 A.U. represents the long-term average of in situ space probe measurements (*7*). The upper line in Fig. 2A gives the RAE density scale. The circles represent the densities determined from the radio positions, if they are placed at the distance of closest approach and it is assumed that the radio radiation occurs at the fundamental of the plasma frequency. The squares in this figure represent the measured densities, if we assume that the radio emission occurs at the second harmonic of the plasma frequency.

Theoretical treatments of the emis-

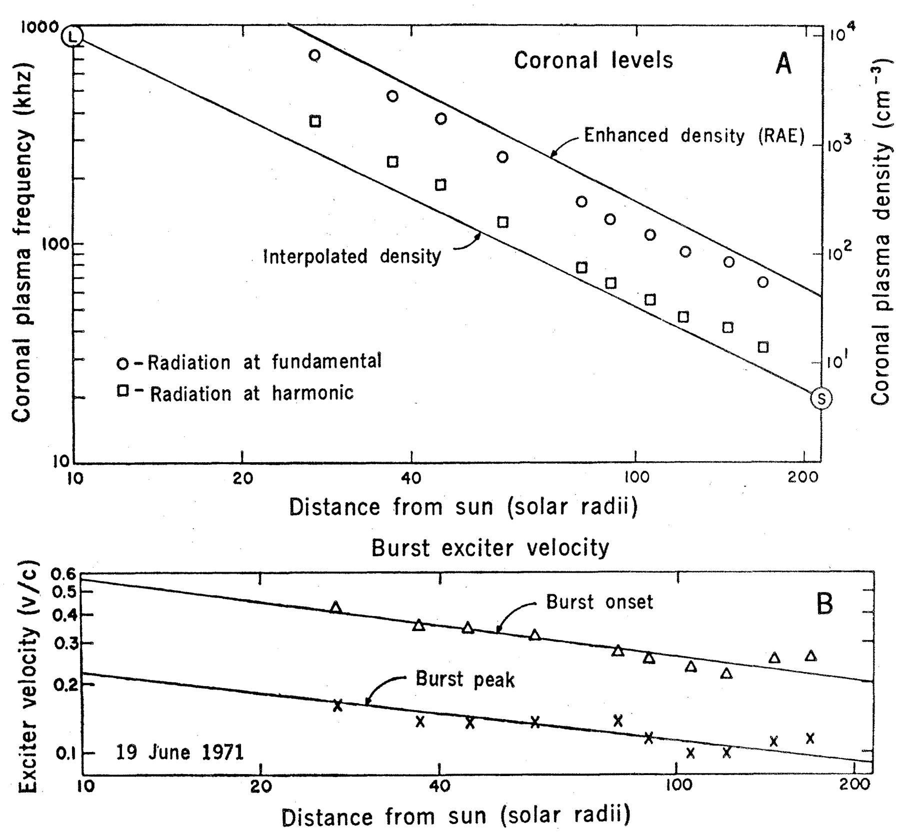

Fig. 2. (A) Coronal density levels in the solar wind expressed in plasma frequency or plasma density plotted against distance from the sun. The interpolated density is given by the line between the measured values L (light scattering) and S (space probe average). The points labeled by circles and squares correspond to values along the trajectory of closest approach for radio emission at the fundamental and second harmonic, respectively, of the plasma frequency. (B) Average burst exciter velocity (v), divided by the velocity of light (c), as a function of distance from the sun for the trajectory of closest approach. Corrections were made for the travel time of light. The burst onset times yielded the values labeled by triangles and correspond to the faster particles in the exciter. The burst peak times yielded the values labeled by X and correspond to particles producing most of the radio burst energy.

sion process indicate that radiation can occur at both the fundamental and the second harmonic of the plasma frequency (*8*). However, the theories have not been definitive in resolving the question of which process dominates (*9*). For the event shown, the second harmonic interpretation of the radio emission is in much better conformity with the interpolated solar wind densities. If, however, emission occurs at the fundamental, one must explain why the radiation occurs preferentially in density-enhanced inhomogeneities.

From the measured drift time from one frequency to another we can determine the speed of the exciter particles. These data are shown in Fig. 2B. The values used in the upper curve were obtained from the burst onset times corresponding to the fastest particles. The peak times were used in the lower curve, which corresponds more closely to the average velocity in the exciter. Both curves indicate an apparent deceleration of the exciter by a factor of about 2 over distances out to 1 A.U.; this indicates a 75 percent loss in energy.

The measurement of radio arrival directions is a method for obtaining information about remote portions of the interplanetary medium. Additional information would be expected from a study of many bursts of this type. The simultaneous data provided by a second spinning spacecraft could be of great value in defining the actual radio positions.

J. FAINBERG
LARRY G. EVANS
R. G. STONE

Radio Astronomy Branch, Laboratory for Extraterrestrial Physics, NASA–Goddard Space Flight Center, Greenbelt, Maryland 20771

References and Notes

1. E. N. Parker, *Astrophys. J.* **128**, 664 (1958); *Interplanetary Dynamical Processes* (Interscience, New York, 1963), pp. 41–72.
2. J. M. Wilcox, *Science* **152**, 161 (1966).
3. R. P. Lin and K. A. Anderson, *Solar Phys.* **1**, 446 (1967).
4. M. R. Kundu, *Solar Radio Astronomy* (Interscience, New York, 1965), pp. 50–64.
5. J. Fainberg and R. G. Stone, *Solar Phys.* **17**, 392 (1971).
6. R. Michard, *Ann. Astrophys.* **17**, 429 (1954); D. E. Blackwell, *Mon. Not. Roy. Astron. Soc.* **116**, 57 (1956); D. E. Blackwell and A. D. Petford, *ibid.* **131**, 399 (1966).
7. A. J. Hundhausen, *Space Sci. Rev.* **8**, 690 (1968).
8. V. L. Ginzburg and V. V. Zheleznyakov, *Sov. Astron. AJ* **2**, 653 (1958); S. A. Kaplan and V. N. Tsytovich, *ibid.* **11**, 1956 (1968); D. F. Smith, *Advan. Astron. Astrophys.* **7**, 147 (1970).
9. V. V. Zheleznyakov and V. V. Zaitsev, *Sov. Astron. AJ* **14**, 47, 250 (1970).
10. L.G.E. is a NAS-NRC postdoctoral resident research associate.

20 July 1972

Mercury: Surface Composition from the Reflection Spectrum

Abstract. *The reflection spectrum for the integral disk of the planet Mercury was measured and was found to have a constant positive slope from 0.32 to 1.05 micrometers, except for absorption features in the infrared. The reflectivity curve matches closely the curve for the lunar upland and mare regions. Thus, the surface of Mercury is probably covered with a lunar-like soil rich in dark glasses of high iron and titanium content. Pyroxene is probably the dominant mafic mineral.*

The spectral reflectivity of the integral disk of Mercury was determined at two different times for the spectral region 0.32 to 1.05 μm. The first measurements were made on the afternoon and evening of 25 December 1969 by using the 60-inch (152.4 cm) telescope of the Cerro Tololo Interamerican Observatory, La Serena, Chile. A dual-beam photometer was used in a sky-subtraction mode with a cooled S-1 photomultiplier tube (ITT model FW-130) and an analog synchronous detection data system (*1*). A set of 22 narrow-band interference filters (200 to 500 Å bandwidth) spaced evenly across the spectral region was used to scan the spectrum (*2*). The star 29 Psc was observed from near twilight until it reached a zenith angle greater than that for the last of the four observations of Mercury. The phase angle of Mercury was 70°.

The second set of measurements was obtained during evening twilight on 12 March 1972 by using the 36-inch (91.44 cm) number 2 telescope of the Kitt Peak National Observatory, Kitt Peak, Arizona. The dual-beam photometer was used in the same mode as in the earlier measurements, with the same photomultiplier tube and filter set. A pulse-counting digital data system was used. The integral disk of Mercury was measured six times alternately with the star ξ^2 Ceti. The phase angle of Mercury was 84°.

Both sets of data were reduced in the same way. Curves of intensity plotted against air mass were prepared for each object, for each filter. For each measurement of Mercury, the ratios of the intensities for Mercury to those for the star at equal air mass for each filter were calculated. The Mercury/star intensity ratios were multiplied by star/sun flux intensity ratios (*2*) to produce reflectivities at each effective filter wavelength (*2*). The values were scaled to unity at 0.564 μm to produce a normalized spectral reflectivity curve for Mercury for each night's observations (Fig. 1). The flux values and reflectivities are available from the authors.

The two measurements shown in

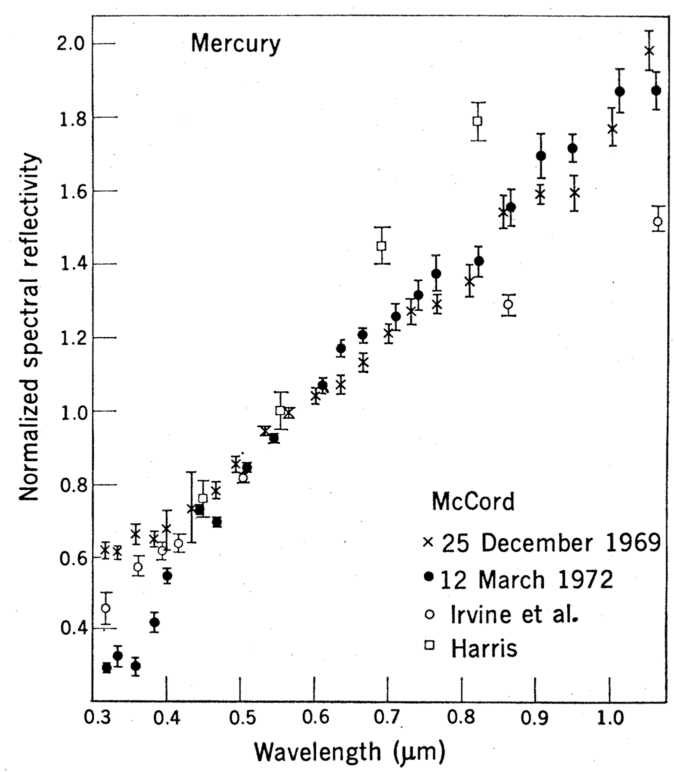

Fig. 1. Spectral reflectivity of the integral disk of Mercury scaled to unity at 0.564 μm for each of two observations. The wavelength position for each point is the same for both data sets, but the 1972 points (filled circles) are offset to the right from the 1969 points (crosses) to make the error bar visible. Also shown are the results of Irvine *et al.* (*3*) and Harris (*4*).